Journal of Thermal Analysis and Calorimetry, Vol. 81 (2005) 169–177

COMPARISON OF ENTHALPY RELAXATION BETWEEN TWO DIFFERENT MOLECULAR MASSES OF A BISPHENOL-A POLYCARBONATE

Pearl Lee-Sullivan[1*] *and M. Bettle*[2]

[1]Department of Mechanical Engineering, 200 University Avenue West, University of Waterloo, Waterloo ON, Canada N2L 3G1
[2]Department of Mechanical Engineering, University of New Brunswick, P.O. Box 4400, Fredericton NB, Canada E3B 5A3

The present work is an extension of an earlier study that compared the stress relaxation between two molecular masses of a bisphenol-A polycarbonate due to thermal aging. The enthalpy relaxation of the same materials has been characterized. First, by measuring the change in enthalpy loss (ΔH_a) and fictive temperature (T_f) as a function of aging temperature (T_a) ranging from –25 to 120°C, using differential scanning calorimetry. For the limited aging time of 120 h, ΔH_a and T_f changes were only appreciable for (T_g *–70 K*)<T_a<T_g . While the influence of molecular mass was somewhat discernible, enthalpy measurements were not as sensitive as stress relaxation tests in differentiating molecular mass effects. In a second investigation, the kinetics of enthalpy relaxation upon isothermal aging at 130°C was evaluated using the peak shift method and found to be comparable to literature values. The plot of ΔH_a as a function of log (aging time) showed two distinct regions: a brief non-linear portion (less than 1 h aging) which is followed by a linear relationship as typically reported in the literature. In contrast to the linear region, the non-linear relaxation behaviour of the poorly aged state does not appear to be dependent on molecular mass.

Keywords: *annealing, enthalpic relaxation, fictive temperature, heat-aging, physical aging*

Introduction

The subject of structural recovery due to physical aging of glassy polymers has been studied extensively over the years because of the profound effects of aging on polymer physical and mechanical properties [1–12]. A common practice in these studies is to heat-age/anneal the polymer at elevated temperatures near glass transition, T_g. Since the early work of Petrie [13], it was recognized that the times required for relaxation of the enthalpy to that of the equilibrium is extremely long, even at temperatures on the order of 15 K below the glass transition, T_g. Hence, thermal aging/annealing at temperatures very near the T_g has been universally applied for studying polymer relaxation kinetics – the thermal treatment is implicitly assumed to represent physical aging.

The purpose of thermal treatment is to accelerate inherent structural recovery processes so that aging experiments can be conducted at shorter timescales. Although it is widely accepted that aging results in changes in the polymer structure and properties, the underlying mechanisms responsible for the changes are still being debated. It has been proposed in our earlier paper [14] that the two main schools of thought on the dominant mechanisms responsible for material property changes in polycarbonate, i.e., free volume recovery *vs.* molecular conformational reorientation, may be reconciled if one interpretes data based on different molecular mechanisms operating at different temperature regimes. Our results are consistent with our collaborators [15, 16] which strongly indicate that heat-aging/annealing are higher activation processes and as such, cannot accurately represent physical aging that occurs at ambient temperature. This supports earlier views by Bauwens [9] and Heymans [10] but the difference in kinetics of the two processes has yet to be established.

Most of the studies on structural relaxation kinetics have attempted to correlate the decrease in measured thermodynamic quantities, namely volume and enthalpy during aging, with mechanical response such as creep and yielding, since these parameters are convenient to measure. There is also growing interest in correlating the ratio of enthalpy to volume relaxation with the apparent bulk modulus of glassy polymers [17].

For polycarbonate in particular, our understanding of its relaxation processes has evolved over the years as more experimental data become available. Early work by Bauwens–Crowet and Bauwens [18] proposed that the kinetics of both yielding and aging (near T_g) processes are identical to enthalpy relaxation, and attempted to link them using the classical

* Author for correspondence: pearls@uwaterloo.ca

1388–6150/$20.00

Akadémiai Kiadó, Budapest, Hungary
Springer, Dordrecht, The Netherlands

WLF and Eyring theories based on free-volume concepts. However, experimental data by Washer [12] showed no correlation between enthalpy relaxation and specific volume, and established that the evolution of enthalpy and mechanical properties cannot be linked to a decrease in free volume. Huu and Vu-Khanh [16] also reported that the variation of yield stress with loading rate and aging time are controlled by two different kinetics. Hutchinson *et al.* [6] and Delin *et al.* [7] contended that the time scales for aging are generally different as monitored by dynamic mechanical, enthalpic and dilatometric techniques, leading to different aging rates. Hence, it is not possible to relate in a simple way the physical aging responses among the different probing methods. To complicate matters further, for the same probing techniques, different analyses can lead to greatly different interpretations of data. Ho and Vu-Khanh [19] showed how two different analytical procedures of the same data set produced by differential scanning calorimetry can lead to very different conclusions.

As the volume of conflicting research work in the literature grows, it is becoming increasingly evident that the details of the physical molecular mechanisms responsible for structural recovery remain unclear. Whether physical aging and annealing/heat-aging are indeed two different processes is still very much open to debate. It is possible that some of the uncertainty may be attributed to the use of different molecular masses of bisphenol-A polycarbonate studied. More comprehensive and systematic characterization of the same resin system would be needed to alleviate some of the confusion.

The present work is an extension of our earlier work [14] which characterized the stress relaxation behaviour of two molecular masses of heat-aged Makrolon bisphenol-A polycarbonate. The interest here is to characterize the enthalpic relaxation of the same two resins for the same aging period of 120 h (5 days) but for wider temperature range, from –25°C to T_g. In addition, a separate set of experiments is also conducted to determine the apparent activation energy for enthalpy relaxation for these materials using the well-recognized phenomenological Tool–Narayanaswany–Moynihan [20–22] or TNM model. Fitted parameters for that model will be compared with literature results for different molecular masses and types of bisphenol-A polycarbonate.

Experimental

Materials

The two types of unmodified Makrolon polycarbonate used in the entire research program were supplied by Bayer Corp.. Rectangular bars of high-molecular mass (HMW) Makrolon 3208 (manufacturer's quoted M_W~32,000) and lower-molecular mass (LMW) Makrolon 2608 (M_W~26,000) were injection-molded by the Polymers Division at Bayer Corp., Pittsburgh. The bar specimens had nominal dimensions 3.12 mm thickness, 12.85 mm width and 152.5 mm length. The HMW-PC specimens were molded at 300°C and 138 MPa (20,000 psi) injection pressure while the LMW-PC were molded at 282°C and 82.8 MPa (12,000 psi). The specimens were shipped in sealed plastic bags and stored in a dessicator before preparation for DSC measurements.

Instrument and specimen preparation

Enthalpy relaxation measurements were performed using a TA Instruments 2920 Differential Scanning Calorimeter (DSC) with a controlled cooling accessory. The temperature scale and cell constant were calibrated with the melting transitions of indium which is the standard procedure. Sapphire was used to calibrate the cell coefficient for heat capacity measurements. Also, the baseline calibrations with an empty cell were performed at regular intervals. The DSC instrument has been rated to have ±0.1°C and calorimetric sensitivity of ±2.5%. Nitrogen was used as the purge gas at a flow rate of 50 mL min^{-1}.

Small samples having approximate dimensions 5×1×3.1 mm were cut off from the bars using a utility knife. Each sample was weighed using a micro- balance before encapsulation in aluminum pans. Initially, all the LMW-PC and HMW-PC samples were heated in the DSC cell for 15 min at 160 and 165°C, respectively. Heating just above the glass transition (T_g=142 and 146°C, respectively) is the accepted method for erasing previous thermal history due to injection molding and any mechanical strain resulting from cutting.

Two separate sets of heat-aging conditions were performed after the thermal erasure treatment. In the first set of tests to study aging temperature dependence (Set I), the samples were cooled at 10 K min^{-1} to the heat-aging or annealing temperature, T_a. Samples were aged at eight different temperatures, T_a= –25, 0, 23, 40, 60, 80, 100 and 120°C, for 120 h or 5 days. Due to the long aging time, the samples to be aged above ambient temperature were removed from the DSC cell immediately upon cooling to T_a , and loaded into a cylindrical steel block pre-heated at T_a. The block ensured temperature stability during the very brief transfer from the DSC to a nearby electrically heated oven controlled to within ±0.2°C. The samples aged at sub-ambient samples were encapsulated in standard aluminum pans and then placed in dou-

ble-sealed plastic bags before aging in controlled freezers set at 0 and –25°C, respectively.

In the second batch of tests to quantify the kinetics of enthalpy relaxation (Set II), encapsulated samples were aged at 130°C (~T_g –15 K for LMW-PC) for up to 2100 h for LMW-PC and 450 h for HMW-PC. Starting from aging time t_a=1 min, samples were periodically taken from the batch for scanning.

Enthalpic relaxation measurements

For samples aged at sub-ambient temperatures, each was loaded onto the DSC for scanning from room temperature. However, samples aged at higher temperatures were quickly re-loaded onto the DSC cell set at the sample aging temperature, T_a. The same procedure was used for each sample to ensure controlled thermal treatments throughout. The sample was then immediately reheated at nominal 10°C min^{-1} to 180°C to obtain the first scan (heat-aged). The same sample was then cooled at 10°C min^{-1} to T_a and re-heated at 10°C min^{-1} to 180°C to obtain the second scan (un-aged reference).

For Set II samples which were aged at 130°C, a down-temperature jump at 10°C min^{-1} to 60°C was included in the procedure prior to the 10°C min^{-1} heating scan for the first aged heating scan. The reference scans for these specimens were also cooled to 60°C before reheating. This was done to ensure that there was a steady heating rate near the glass transition temperature since there are fluctuations during initial heat-up as the controller tries to attain the set ramp.

Data analysis

The sequence of enthalpy changes in the glassy PC sample as it is subjected to the various thermal treatments, is depicted in Fig. 1. Point c represents a sample with thermal history erased – at above T_g, the polymer readily achieves equilibrium. As the sample is cooled to T_{gc}, it follows the equilibrium cooling line. But below T_{gc}, the enthalpy of the sample departs from equilibrium – the higher the cooling rate, the greater the departure. As the sample departs further from equilibrium (moving towards point a), it increases in excess enthalpy. When cooling stops at the aging temperature, T_a, (point a) the polymer has an excess enthalpy equal to ΔH_o. During the aging treatment itself, going from points *a* to *b*, the excess enthalpy is reduced by the amount ΔH_a – the longer the aging time, the greater is ΔH_a. Accordingly, the magnitude of ΔH_a is a strong function of the thermal path [23]. This phenomenon is commonly termed as enthalpy relaxation.

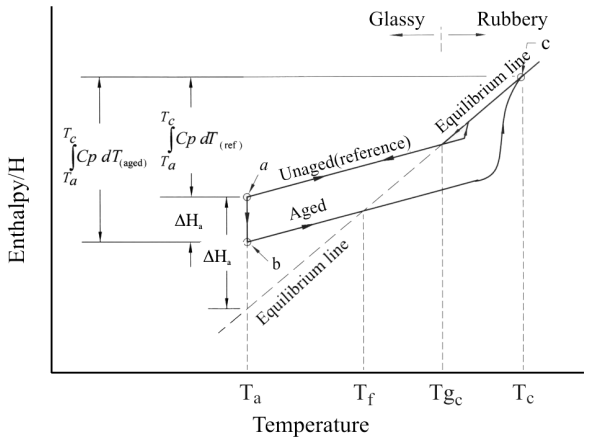

Fig. 1 Schematic diagram depicting the sequence of enthalpy changes when the polymer is subjected to various thermal treatments

Upon reheating from point *b* to obtain the first scan (heat-aged), the enthalpy of the sample crosses the equilibrium line at the fictive temperature, T_f, which identifies the structural state of the glass. T_f is discussed later in this paper.

Determination of enthalpy loss

Most of the published work in the literature utilize the method proposed by Petrie [13], to find the enthalpy loss on aging, ΔH_a, which is simply the area difference under the DSC heat flow curves for the aged and for reference scans. The heat flow curves can be converted to corresponding total heat capacity C_p curves by dividing the heat flow per unit mass values by the instantaneous underlying heating rate

$$C_p = \frac{Heat\ flow\ per\ unit\ mass}{underlying\ heating\ rate}$$

The underlying heating rate measured in our experiments is 10.2°C min^{-1}. The enthalpy loss during aging, ΔH_a, is then found by the difference in integration of aged and reference curves of C_p *vs.* temperature between the aging temperature, T_a, and the temperature at which both the aged and reference samples attain equilibrium above the glass transition, T_c, Fig.1:

$$\Delta H_a = \int_{T_a}^{T_c} (C_p)_{aged}\,dT - \int_{T_a}^{T_c} (C_p)_{ref}\,dT \qquad (1)$$

Determination of fictive temperature

The concept of a fictive temperature, T_f, was developed by Tool [20, 24, 25] who proposed that the relaxation kinetics of a non-equilibrium glassy structure depended not only on temperature but also upon the instantaneous state or the structure of the glass during the relaxation. Since the kinetics of aging and the glass transition are non-linear, T_f is a convenient pa-

rameter for comparing the different states of the same glassy polymer if the same thermodynamic property, such as enthalpy or volume, is used. In this work, the observed T_f is defined as the temperature at which the observed enthalpy would be the equilibrium value.

The values of T_f were determined using the TA Universal Analysis 2000® software. Although not indicated in the instrument manual, the technique used is that proposed by Richardson and Savill [26] for the determination of the so-called equilibrium glass transition. In this method, Fig. 2, the rubbery enthalpy line is extrapolated back to the point where it intersects the glass enthalpy line (heat-up curve). It was found, however, that the value was somewhat sensitive to the temperature limits used in the analysis. They were thus compared with the T_f values determined using the better known 'equal area method' by Moynihan *et al.* [22]. Since both values were almost identical, the software values have been plotted in our results.

Determination of TNM model parameters

The so-called TNM equation [20–22] has been adopted in this work. This phenomenological equation assumes that the relaxation time τ for enthalpic relaxation depends on both the temperature (T) and the fictive temperature, T_f, as shown in the expression

$$\tau = \tau_o \exp\left[\frac{x\Delta h^*}{RT} + \frac{(1-x)\Delta h^*}{RT_f}\right] \quad (2)$$

where τ_o is the value of τ in equilibrium at infinitely high temperature, Δh^* is the apparent activation energy for enthalpy relaxation, R is the gas constant, and $x(0 \leq x \leq 1)$ is the nonlinearity parameter [27, 28] identifying the relative contributions of temperature and structure of the relaxation time(s).

Following [22], the apparent activation energy Δh^* has to be determined using a separate set of so-called constant cooling rate experiments. In this work, the experiment consisted of heating past T_g and cooling at different cooling rates, i.e., 0.2, 0.5, 2.5, 5, 10 and 20°C min^{-1}, to 60°C before immediately scanning at 10°C min^{-1} past T_g. The same sample was used for each molecular mass PC. The dependency of T_f on the cooling rate, q_1 , may be written as:

$$\frac{d[\ln(q_1)]}{d[1/T_f]} = -\frac{\Delta h^*}{R} \quad (3)$$

The apparent activation energy is then evaluated from the slope of a plot of $\ln[q_1]$ *vs.* $[1/T_f]$.

In this work, the non-linearity parameter, x, has been analyzed using the so-called peak shift method as described in [6]. As for Δh^*, the procedure for evaluating x is also described in great detail in that paper. Results from fitting the TNM model for extruded Lexan polycarbonate (M_w=31,000) were reported and the peak shift analysis was rigorously compared with other empirical approaches [29, 30]. The method was considered more reliable than [30] for analyzing large departures from equilibrium on heating.

For a set of experiments, the cooling rate (q_1), the heating rate, (q_2) and T_a are fixed while t_a is varied. The non-linearity parameter, x, is found by first determining the so-called dimensionless shift $\hat{s}(D)$ given by

$$\hat{s}(\overline{D}) = \Delta C_p \left(\frac{\partial T_p}{\partial \Delta H_a}\right)_{q_1, T_a, q_2} \quad (4)$$

where T_p is the peak temperature of the endotherm and $\Delta C_p = C_{pl} - C_{pg}$ is the difference between the specific heat capacities of the equilibrium liquid and the glass. The right-hand side of the equation may be evaluated by

$$\Delta C_p \frac{\partial T_p}{\partial \log(\text{aging time})} \Big/ \frac{\partial \Delta H}{\partial \log(\text{aging time})} \quad (5)$$

Although Eq. (2) provides a formal procedure for analyzing DSC scans, it can only describe the kinetics of enthalpy relaxation for a single relaxation time. Dynamical processes in disordered materials exhibit relaxation patterns that follow a distribution of relaxation times. One of the more common models used for modeling continuous behaviour is the Kohlrausch–Williams–Watts (KWW) or the stretched exponential response function [31, 32], $\phi(t)=\exp[-(t/\tau)^{\beta}]$ which uses the τ given in Eq. (2) to predict the shape of the continuous spectrum. The non-exponentiality of the recovery process is defined by β ($0 \leq \beta \leq 1$) which is also referred to as the shape parameter since it is inversely related to the width of the spectrum. It was found in our earlier statistical analysis work [33] that β is a repeatable indicator for characterizing thermal aging effects in stress relaxation tests.

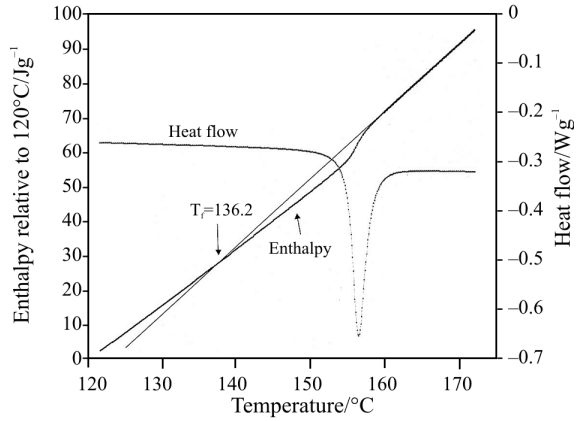

Fig. 2 The determined fictive temperature is the intersection point of the extrapolated rubbery enthalpy line and the glass enthalpy line

Table 1 Comparison of TNM parameter values

Reference	PC tradename or supplier	Molecular mass	$\left(\frac{\partial \Delta H_a}{\partial(\log(t_a))}\right)_{q_1,T_a,q_2}$ /J g^{-1} per decade	$\frac{\Delta h^*}{R}$ / kK	x	ΔC_p / J g^{-1} K^{-1}
Bauwens Crowet and Bauwens [18]	Makrolon	M_v=26,000	0.62	–	–	0.234
This work	Makrolon	M_w=26,000	0.63	136±28	0.43	0.259±0.014
Hutchinson *et al.* [6]	Lexan	M_w=31,000	0.67	140	0.46±0.2	0.258±0.006
This work	Makrolon	M_w=32,000	0.53	157±8	0.40	0.252±0.02
Hodge [29]	Aldrich	M_w=33,800	–	150 ±15	0.19	–

M_v – viscosity-average molecular mass, M_w – mass-average molecular mass

Results and discussion

Dependence of ΔH_a and T_f on T_a

Typical C_p curves for Set I samples of LMW-PC and HMW-PC aged at increasing temperatures are plotted in Figs 3 and 4, respectively. Some of the curves were shifted vertically to align them with the baseline. Lower temperatures have not been included since they exhibit very similar behaviour to 60°C . As expected, greater relaxation is attained at higher temperatures. The enthalpy loss on aging, ΔH_a , determined from Eq. (1) for the various aging temperatures is plotted in Fig. 5. Each aged condition scan was repeated once and results for the two tests have been plotted. The temperature range used for the analyses are 140 and 165°C . As seen in Fig. 5, the data pairs are very close with differences of about 0.1 J g^{-1}. The highest difference was found for HMW-PC aged at 100°C was 0.13 J g^{-1} or 14% difference.

The enthalpy losses for LMW-PC and HMW-PC in Fig. 5 are not appreciable for samples aged at temperatures (T_a) below 75 and 80°C , respectively. Since T_{gc} is dependent on heating rate, we assigned the fictive temperature for the reference scan as the glass transition temperature, T_g, which corresponds to 142 and 146°C for LMW-PC and HMW-PC, respectively.

If the same results in Fig. 5 are plotted in terms of T_g–T_a, the detectable interval is (T_g–70*K*)<T_{detect}<T_g, as shown in Fig. 6. Within this region, there is a sharp linear increase in enthalpy loss with increasing T_a. When T_a is less than (T_g–70 K*),* the relaxation rate is too slow to be discernible; the aging time of 120 h is short compared to the relaxation times at those temperatures. Our present results appear to agree with the theoretical model prediction by Bauwens-Crowet and Bauwens [18] for the aging time of 120 h (ln*t*=4.8). Their model predicts the dependence of ΔH_a on a structural temperature parameter, θ, rather than the aging temperature. θ is defined as the temperature at which the structure of a sample in metastable state would be in equilibrium, and is supposed to fully

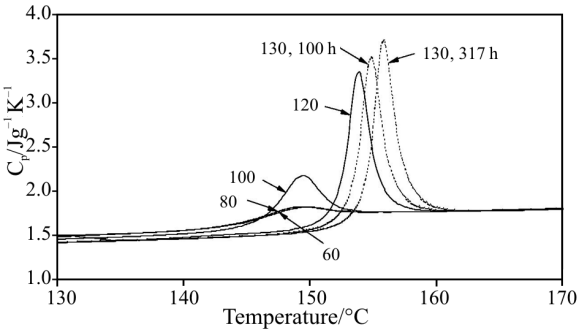

Fig. 3 Typical heat capacity (C_p) curves for LMW-PC aged for 120 h at various temperatures

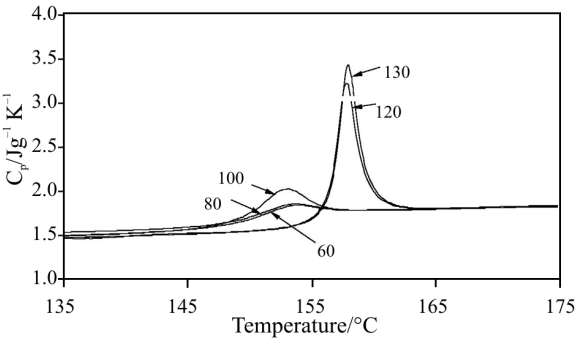

Fig. 4 Typical heat capacity (C_p) curves for HMW-PC aged for 120 h at various temperatures

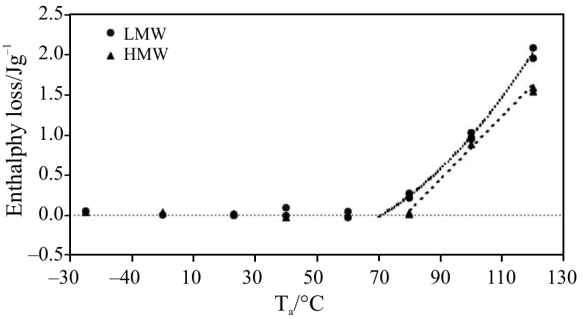

Fig. 5 Enthalpy loss for aged HMW and LMW polycarbonate as a function of aging temperature, T_a. All samples were aged for 120 h

characterize the structural state of the sample. According to the model, at constant aging temperature, T_a, of the order of T_g – 15 K, it can be assumed that T_a=θ. It is interesting that if we extrapolate Fig. 2 in [18] to aging time of 120 h (ln$t$=4.8), the model is still able to predict the onset of an appreciable enthalpic loss at temperatures as low as T_g–70 K.

In both Figs 5 and 6, the enthalpy losses for LMW-PC are slightly higher than HMW-PC indicating higher or faster structural recovery occurred in LMW-PC due to its inherent shorter chain and greater amount of end-groups and slightly higher free volume. The observation is consistent with our stress relaxation results [14] which were explained by well-established bulk free volume recovery concepts. However, in comparing the two probing methods, the influence of molecular mass was better differentiated in stress relaxation. The present results also agree well with the yielding results by [16], that the decrease in entropy is more important for the lower molecular mass polycarbonate. When all the results are viewed together, it becomes clear that molecular mass effects are more easily differentiated in mechanical tests than in enthalpy measurements.

Correspondingly, the plot of change in fictive temperature, ΔT_f, in Fig. 7 also shows that a rise occurs only for T_a greater than 75°C or (T_g –70K) and that there is

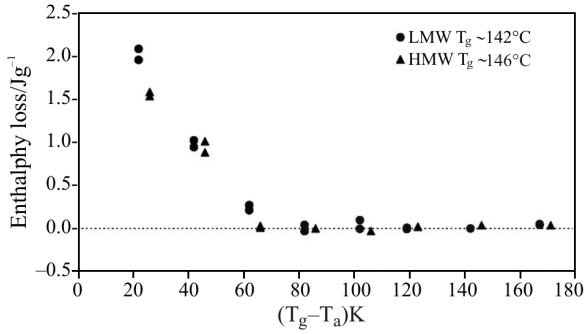

Fig. 6 Enthalpy loss for aged HMW and LMW polycarbonate data in Fig. 5 re-plotted as a function of (T_g – T_a)

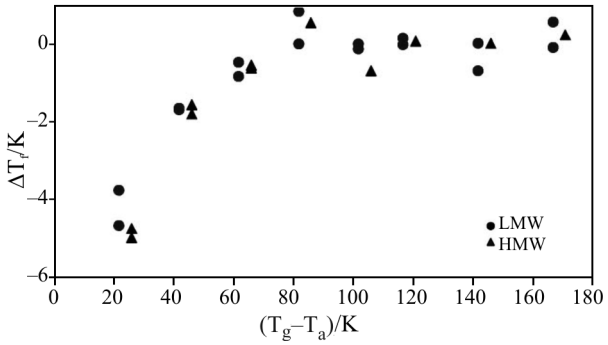

Fig. 7 The change in fictive temperature as a function of (T_g – T_a) after aging for 120 h

negligible difference in the structural state below that temperature. The experimental scatter appears to be larger for the poorly aged samples. As expected, the fictive temperature for HMW–PC is generally higher than LMW-PC, and ΔT_f is the highest for the highest T_a. However, in contrast to enthalpy loss, the fictive temperature change is non-linear.

Analysis of TNM model parameters

DSC data from scanning Set II samples was curve fitted to determine the TNM model parameters using the analytical procedures described in ref [6]. Accordingly, the present results are compared with those of ref. [6] and also two other sources quoted in the literature [18, 30] in Table 1. For easier comparison, the polycarbonates are listed in ascending order of molecular mass.

*Apparent Activation Energy, Δh**

Using data from cooling rate experiments for both materials, the slopes of the ln [q_1] *vs.* $1/T_f$ plots were determined using least-squares best fit method and are shown in Table 1. It is seen that the value of $\Delta h^*/R$ for HMW-PC is higher than that for LMW-PC. The apparent activation energy, Δh^*, evaluated from Eq. (3) is 1130±240 kJ mol^{-1} for LMW-PC and 1310 kJ mol^{-1}±70 kJ mol^{-1} for HMW-PC, with uncertainties based on a 95% confidence interval for the slopes. The higher activation energy for HMW-PC agrees with our earlier stress relaxation results which showed that stress relaxation rates at high temperatures are strong functions of molecular mass. HMW-PC has lower mobility than LMW-PC and requires a higher degree of cooperative segmental motion. Although our results are consistent with expected molecular mass effects, Table 1 suggests that molecular mass effects cannot be directly deduced by comparing different types of bisphenol-A polycarbonate.

Non-linearity coefficient, x

The dependency of enthalpy loss on the logarithm of aging time for isothermal aging of the Set II samples at 130°C is shown in Fig. 8. As anticipated, a linear increase of ΔH_a with log (aging time) is seen for much of the curve but the relationship is non-linear for aging times less than 1 h (log t=0). The slopes of the best least-squares fit straight lines from t_a=1 h onwards are 0.629 and 0.526 J g^{-1} per decade for LMW-PC and HMW-PC, respectively. The correlation coefficients are 0.975 and 0.971 respectively. As shown in Table 1, the LMW-PC value is close to that obtained by [6] for a higher molecular mass Lexan-PC.

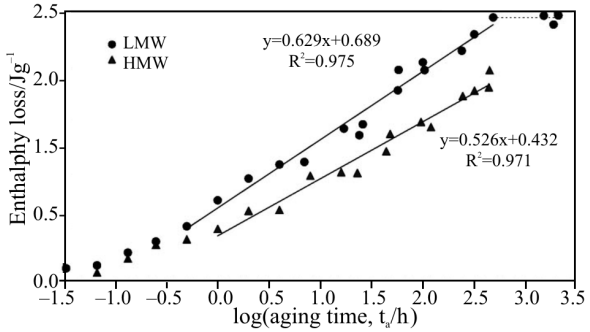

Fig. 8 Dependence of the enthalpy loss during isothermal aging at 130°C as a function of log[aging time] for both polycarbonates. The straight lines show the best least-squares fit of data aged ≥2 h

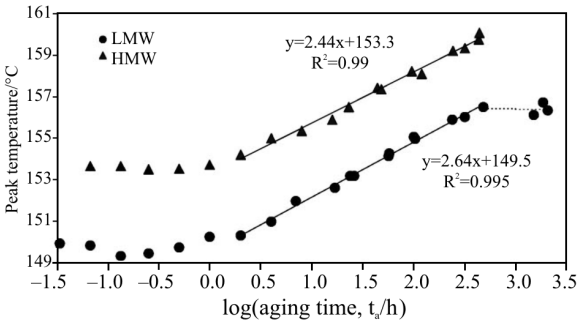

Fig. 9 Dependence of endothermic peak temperature on log[aging time] for both polycarbonates samples aged at 130°C. The straight lines show the best least-squares fit of data aged ≥2 h

The small but discernible enthalpy loss at very short aging times has yet to be reported in the literature. Our data start at t_a=1 min or 0.0167 h (log t= – 1.77) for LMW-PC. Both polycarbonates appear to follow a very similar non-linear rate before diverging at t=1 h. Results by Ho and Vu-Khanh [19], using the same HMW-PC, also appear to miss this early aging stage since the range was not investigated. However, their enthalpy measurements at 80°C suggest that rejuvenation dominates aging processes at short aging times and/or lower aging temperature leading to a net gain in enthalpy.

The present results imply that the widely accepted use of the ΔH_a/log (aging time) slope for evaluating TNM parameters can only describe the enthalpy relaxation of highly aged states. The higher slope for LMW-PC is consistent with the expected higher rate of linear volume relaxation. However, the initial relaxation rates in Fig. 8 do not appear to be influenced by molecular mass effects. This raises the question as to whether the non-linear behaviour of poorly aged states, even near T_g, can be modeled by simple free volume concepts. It is also unclear how the non-linear behaviour within the interval ($0<t_a<1$ h) is related to the energy absorbed due to rapid conversion from high-energy *trans-cis* conformation to lower energy *trans-trans* conformation. Lu *et al*. [34] reported that the conformational change when annealing polycarbonate near T_g is abrupt and that the energy absorbed during the step conformational change after annealing at 127°C for 48 h is 0.15 J g^{-1}. Although the energy absorbed is expected to represent only a fraction of the DSC endotherm, it is interesting that the order of the step change is close to our values measured within the few minutes of aging tests.

When we performed additional aging experiments for LMPW-PC to explore longer aging times, the enthalpy loss did not vary much for log(t_a)>3.0, as in Fig. 8. Results published by [6] show a linear dependency of ΔH_a on log(t_a) beyond that temperature while [19] did not study such prolonged aging times. There is insufficient aging data to be conclusive but this observation may be related to the apparently unusual self-limiting relaxation behavior that is specific to polycarbonate [35, 36]. More aging studies conducted at different aging temperatures and at much longer aging times are necessary to confirm this.

The dependence of the heating scan peak endothermic temperature, T_p, on log(t_a) is shown in Fig. 9 for the two materials. The slopes of the best-fit straight lines are 2.64 and 2.44 K per decade for LMW-PC and HMW-PC, respectively, with corresponding correlation coefficients of 0.995 and 0.990. The invariance of T_p at short aging times that has been shown theoretically elsewhere [37, 38] is also observed here. However, we also see that T_p is no longer linearly dependent on log(t_a) when log(t_a)>3.0. When the slopes of both curves in Figs 8 and 9 are combined, $\frac{\partial T_p}{\partial \Delta H_a} = 4.20$ and 4.63 g K J^{-1} for LMW-PC and HMW-PC respectively.

The values for ΔC_p were evaluated following the procedure outlined in ref. [6]. C_{pg} was taken at T_f of the reference curves (q_1=q_2=10°C min^{-1}) and C_{pl} was taken at the beginning of the baseline section immediately after the endothermic peak, T_p. The average values from ten measurements gave ΔC_p=0.259±0.014 and 0.252±0.02 J g^{-1} K^{-1} for LMW-PC and HMW-PC, respectively. Again, as seen in Table 1, these values are comparable to literature reports.

The dimensionless shift values for LMW-PC and HMW-PC, evaluated using Eq. (4), are 1.09 and 1.17 respectively. By reading off the master curve for the dimensionless shift in Fig. 3 of [6], the x values are approximately 0.43 and 0.40. The expected error in that estimate should be similar to [6] who found x to be 0.46±0.02. In Table 1, Hodge [30] found x=0.19 using a non-linear curve fitting method but this discrepancy has been attributed by [6] to be due to the analysis per-

formed on conditions too close to equilibrium and is insufficiently nonlinear.

Finally, the β parameter of the stretched exponential was estimated by plotting the parameters C^{N}_{pu} as a function of $\log[q_1/q_2]$ as described in [6]. Our curves were very similar to that shown in [6], but were shifted higher and to the right. Nevertheless, the values of β for both polycarbonates fell within the same range of $0.456<\beta<0.6$, with the HMW-PC having a slightly lower value. Although the curves were much too close to be conclusive, the combined observation of lower β and higher Δh^* for HMW-PC would be consistent with increased chain entanglement/packing and reduced mobility. Again, based on the limits estimated by [6], the values of both HMW and LMW would be closer to the theoretical limit value of $\beta=0.6$ than 0.46.

It is interesting to note that Privalko *et al*. [39] also found dependence of both Δh^* and β on molecular mass but more recent DSC studies by Hernández Sanchez *et al*. [40] on a wide range of molecular masses of polystyrene showed no systematic dependence of β with molecular mass.

Conclusions

The values of the non-linearity parameter, x, determined from the linear dependence of enthalpy loss with log(aging time) were close to those reported in the literature. However, the values only describe aging kinetics for highly aged polycarbonate since the relationship is non-linear at very short aging times even when thermal aging is very close to T_g. If physical aging is considered to be comparable to a poorly aged state (short aging times and/or low aging temperature), this would lend support to the argument that the kinetics of highly aged glassy polymers are different from the physical aging phenomenon.

Although all the TNM model parameters found in this work were very close to those reported in the literature, the influence of molecular mass cannot be deduced by comparing different types of bisphenol-A polycarbonate. When two molecular masses of the same type of material are compared, the observed differences in the TNM parameters are consistent with the well-established cooperativity principles of glass transition kinetics. In comparison with earlier stress relaxation studies, it is evident that enthalpy relaxation measurements are much less sensitive than mechanical tests in differentiating molecular mass effects.

Acknowledgements

The authors wish to thank the Natural Science and Engineering Research Council of Canada (NSERC) for supporting Mr. M. Bettle through an USRA Scholarship. The assistance of Dr. James Chung of the Polymer Division, Bayer Corp., Pittsburgh, for providing the Makrolon samples is gratefully acknowledged.

References

1 M. S. Ali and R. P. Sheldon, J. Appl. Polym. Sci., 11 (1970) 2619.
2 K. Neki and P. H. Geil, J. Macromol. Sci. - Phys., B8, (1–2), (1973) 295.
3 L. E. Struik, Physical Aging in Amorphous Polymers and Other Materials, 1978, Elsevier, Amsterdam.
4 J. Y. J. Chung and N.R. Lazear, Soc. of Plastics Engineer's Annual Tech. Conf., ANTEC 1994, (1994) 1728.
5 J. M. Hutchinson, Prog. Polym. Sci., 20 (1995) 703.
6 J. M. Hutchinson, Macromolecules, 32 (1999) 5046.
7 M. Delin, R.W. Rychwalski, J. Kubat, C. Klason and J. M. Hutchinson, Polym. Eng. Sci., 36 (1996) 2955.
8 F. J. Cama and L. Morbitzer, Proc. Conf. Antec 82', (1982), Society of Plastics Engineers, 96.
9 J.–C. Bauwens, Plast., Rubber Compos. Process. Appl., 7 (1987) 143.
10 N. Heymans, Polymer, 34 (1997) 3435.
11 W. Stolarski, A.Letton, E. Nour and J. Laane, in Proc. Conf. 'ANTEC '94' (1994) Society of Plastics Engineers, 2077.
12 M. Washer, Polymer, 26 (1985) 1546.
13 S. E. B. Petrie, J. Macromol. Sci. - Phys., B12(2) (1976) 225.
14 P. Lee-Sullivan, D. Dykeman and Q. Shao, Polym. Eng. Sci., 43 (2003) 369.
15 C. H. Huu and T. Vu-Khanh, Damage and Fracture Mechanics VI, Selvadurai, A. P. S. and Brebia, C. A., eds., WIT Press , 2000, p. 365.
16 C. H. Huu and T. Vu-Khanh, Theoretical and Applied Mechanics, 40 (2003) 75.
17 A. Slobodian, A. Lengálová and P. Sáha, J. Therm. Anal. Cal., 71 (2003) 387.
18 C. Bauwens-Crowet and J.-C. Bauwens, Polymer, 27 (1986) 709.
19 C. H. Ho and Vu-Khanh, Theoretical and Applied Mechanics, 39 (2003) 107.
20 A. Q. Tool, J. Am. Ceram. Soc., 32 (1946) 240.
21 C. T. Narayanaswamy, J. Am. Cer. Soc., 54 (1971) 491.
22 C. T. Moynihan, A. J. Easteal, M. A. Debolt and J. Tucker, J. Am. Ceram. Soc., 59 (1976) 12.
23 R. R. Lagasse, J. Polym. Sci. Polym. Phys. Ed , 20 (1982) 279.
24 A. Q. Tool and C. G. Eichlin, J. Am. Ceram. Soc., 14 (1931) 276.
25 A. Q. Tool, J. Am. Ceram. Soc., 31 (1948) 177.
26 M. J. Richardson and N. G. Savill, Polymer, 16 (1975) 753.
27 A. J. Kovacs, J. J. Aklonis, J. M. Hutchinson and A. R. Ramos, J. Polym. Sci., Polym. Phys. Ed., 17 (1979), 1097.

28 A. J. Kovacs, J. M. Hutchinson and J. J. Aklonis, In The Structure of Non-Crystalline Solids, P. H. Gaskell, Editor, Taylor and Francis, London, 1977, p. 153.
29 I. M. Hodge, Macromolecules, 20 (1987) 2897.
30 I. M. Hodge, Macromolecules, 16 (1987) 898.
31 F. Kohlrausch, Pogg. Ann. Phys., 12 (1847) 393.
32 G. Williams and D. C. Watts, Trans. Faraday Soc., 14 (1981) 54.
33 D. Dykeman and P. Lee-Sullivan, Polym. Eng. Sci., 43 (2003) 383.
34 J. Lu, Y. Wang and D. Shan, Polym. J., 32 (2000) 3954.
35 R. Wimber-Friedl and J. G. Bruin, Macromolecules, 29 (1996) 4992.
36 C. G. Robertson and G. L. Wilkes, Macromolecules, 33 (2000) 3954.
37 A. R. Ramos, J. M. Hutchinson and A. J. Kovacs, J. Polym Sci., Polym. Phys. Ed., 22 (1984) 1655.
38 J. M. Hutchinson, Lect. Notes Phys., 277 (1987) 172.
39 V. P. Privalko, S. Demchenko and Y. S. Lipatov, Macromolecules, 19 (1986) 901.
40 F. H. Hernández Sánchez, J. M. Meseguer Dueñas and J. L. Gómez Ribelles, J. Therm. Anal. Cal., 72 (2003) 631.

DOI: 10.1007/s10973-005-6993-0